

Particle crushing: passive detection

Sha Luo¹, Andrea Diambra¹, Erdin Ibraim¹

¹*University of Bristol, Senate House, Bristol, BS8 1TH, UK, s113796@bristol.ac.uk,
andrea.diambra@bristol.ac.uk, erdin.ibraim@bristol.ac.uk.*

Abstract: When the confining pressure is sufficiently large, soil grain breakage can occur and this can have a significant influence on the performance of a wide range of geotechnical systems such as shallow foundations, embankments and dams, railway substructures. However, the mechanics of particle crushing still remains one of the most difficult problems in geomechanics, while the link between the breakage of particles and the mechanical response of the soil through adequate continuum constitutive models has not been solved satisfactorily. This study investigates the possibility of using Acoustic Emission (AE) technique to predict the extent of soil particle breakage and its evolution under loading. Insight into the use of AE to characterize the breakage signature of particles is gained through testing of individual glass spherical particles of different sizes. It is shown that the frequency content of the AE breakage signals does not appear to be affected by the particle size and that suggests that the AE can be directly linked to a typical particle breakage mechanism. At the breakage point all the glass particles disintegrate instantly into small pieces.

I. INTRODUCTION

Design of geotechnical systems require continuum models for soils whose response is the result of the fabric and individual particle interactions. Fabric includes all aspects of average particle arrangement and sizes (grading). When the confining pressure is sufficiently large, grain breakage can occur and this can have a significant influence on the performance of a wide range of geotechnical structures such as shallow foundations, embankments and dams, railway substructures [1,2]. However, the mechanics of particle crushing still remains one of the most difficult problems in geosciences. The link between the breakage of particles and the mechanical response of the soil through adequate continuum constitutive models has not been solved entirely satisfactorily.

Acoustic Emission (AE) monitoring technique has been used in various engineering applications. The acoustic emissions are microseismic events that occur on materials - at small sample scale or large structural scale - during loading. The AE events are recorded by a transducer or an array of transducers and the data can complement other

mechanical measurements of stress or strain by providing insight into various internal material phenomena and mechanical interactions. The AE technique is widely used for the assessment of damage and failure of brittle materials [3], evaluation of the response of retrofitted reinforced concrete elements [4], detection of the onset and position of failure in fiber reinforced composite materials [5-8], monitoring of large bridge structures [9]. In geomechanics, pioneering work of Koerner and co-workers [10-13] and more recently [14-17] used the AE technique to assess the stability of soil slopes. Correlations between the characteristics of the acoustic emission in soils subjected to oedometric compression, triaxial testing, cone penetrometer tests, direct shear and deformation properties, including particle crushing have been conducted by [18-23].

This study explores the possibility of using Acoustic Emission (AE) as a passive technique to characterize the extent of soil particle breakage and predict its particle size evolution under loading. For this purpose, insight into the breakage mechanisms of individual particles is gained through mechanical testing under uniaxial compression, while AE particle crushing is systematically recorded. This work presents preliminary experimental results obtained on spherical glass particles of different sizes.

II. MATERIALS

Five different borosilicate glass spherical particle size groups with diameters ranging from 1mm to 6mm supplied by Sigmund Lindner GmbH and described as SiLibeads type M had been tested (Fig.2.1). While a number of approaches to shape description have been proposed in the literature, based on previous QicPic measurements [24] and optical 2D microscope analysis, the particles' aspect ratio, sphericity and convexity parameters [25,26] have been evaluated. The size of the particles has been defined in terms of the equivalent area diameter d_a [27]. d_a is the diameter of the circle which has the same area with the projection area of the particle outlet in the optical microscope. The shape descriptors and the equivalent area diameter are measured on 2D projections of the real 3D particles. These can only be statistically representative if these 2D projections are obtained from particle orientations that are random in 3D [28]. While recognising that such data is not normally

attainable using microscopy, in this study, the shape descriptors and d_a for an individual particle have been evaluated based on three microscope images of the particle placed in different positions on the microscope set up. The values of each of the shape descriptors were consistently larger than 0.95, i.e. the particles were very close to being perfect spheres. The individual average values of d_a for each tested particle, and the resulted averages for each group size are presented in table 2.1. A particle shear stiffness of 16.7 GPa along with a Poisson's ratio of 0.20 were obtained from measurements on representative glass beads [24]. The particle density of the glass beads is 2.23 g/cm^3 .



Fig. 2.1. Picture of five types glass sphere particles

Table 2.1. Mean equivalent area diameter

d _a of glass sphere particles (mm)					
Groups	6mm	4mm	3.5mm	2.5mm	1mm
d _a	6.013	4.071	3.613	2.462	1.047
	5.951	4.037	3.557	2.498	1.071
	5.986	4.111	3.581	2.480	1.059
	5.897	3.976	3.580	2.479	1.136
	5.976	4.098	3.569	2.504	1.138
Mean	5.964	4.059	3.580	2.485	1.090

III. TEST SETTING

A. Equipment

The uniaxial compression test on individual particles uses a displacement controlled electro-mechanical loading frame (Figure 3.1). Each bead was compressed between two rigid steel platens, of which one is fixed to the loading ram that incorporates an LVDT for vertical displacement measurements and a 5 KN-load cell. The lower platen moves upwards with a speed of 0.05 mm/min until the particle crushes. The crushing takes place in a brittle explosive mode.

During the crushing test, two piezoelectric sensors with a bandwidth between 10 kHz and 1 MHz record the acoustic emissions. The first AE sensor (AE 1), which links to channel 1 of the AE acquisition system, is fixed within the steel base plate, just below the particle at a depth about 1 cm, by means of a mechanical system that ensures a constant holding force (Figure 3.1). The second AE sensor (AE 2), which links to channel 2, is simply placed on the base plate at a distance of about 4 cm from the particle. For both sensors, silicon grease is also used as coupler. The typical parameter setting of the AE acquisition system is listed in table 3.1.

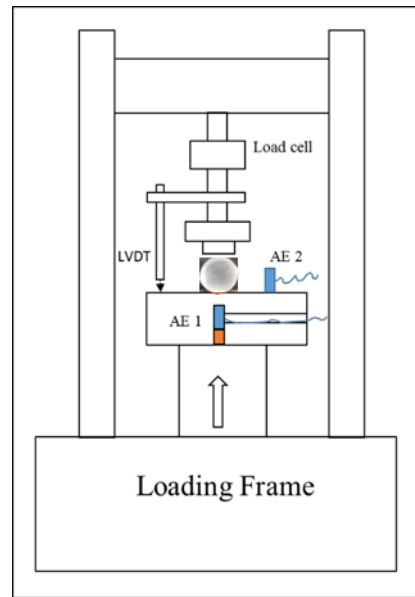


Fig. 3.1. Diagram of loading system

Table 3.1 Typical settings of the AE acquisition system

Sampling rate	5 MSPS
Preamplifier gain	20 dB
Threshold of detection	40 dB
PDT(Peak definition time)	40ms
HDT(Hit definition time)	120ms
HLT(Hit Lockout time)	300ms

B. Data collection

During the crushing test, the resulting vertical force and displacement are recorded, while the AE system allows the acquisition of the acoustic bursts. Figure 3.2 shows a typical AE signal and some associated AE parameters.

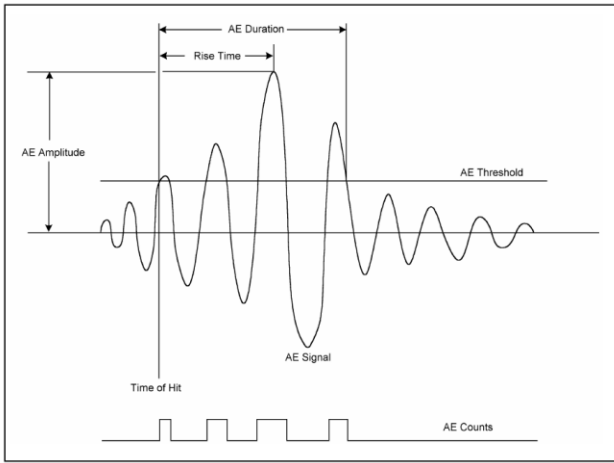


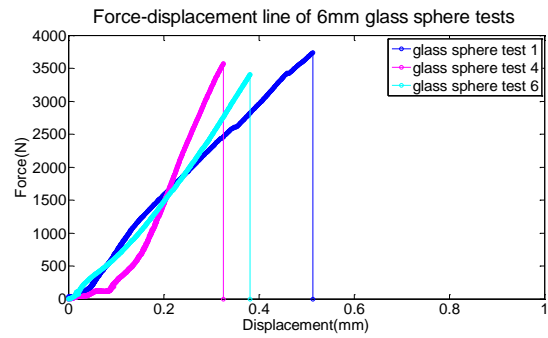
Fig. 3.2. Typical AE burst signal and some associated AE parameters.

IV. RESULTS & DISCUSSION

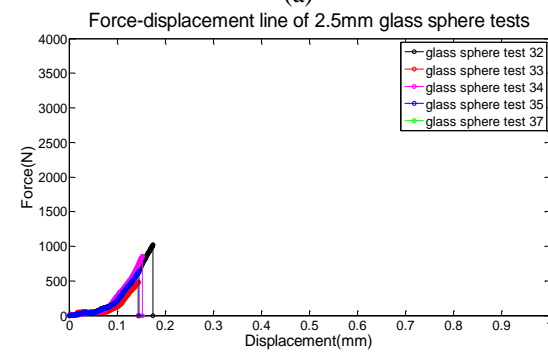
The presentation of the test results is divided into three main sections. First, the observed mechanical response during uniaxial compression is presented, then the associated AE monitoring records are analyzed, and finally, the AE signals corresponding to the crushing events are examined in the frequency domain.

A. Uniaxial compression

Figure 4.1 shows some typical force-displacement responses obtained during the compression tests on two particle groups sizes. It can be seen that after an initial part with a low rate progress, the vertical force increases at a higher rate and remains almost proportional with the vertical displacement until a maximum is reached and a sudden decrease occurs as the particle fully fractures. No partial fracture or detachments of parts of the beads were observed before the final brittle fragmentation. For a given particle size group, some variation of the peak crushing force is clearly observed. While variation of the material properties including internal defects may explain these differences, due to the surface particle-platen and some inherent loading system imperfections, it is also likely that at some stage frictional sliding of the particle occurred. As discussed by [29], in this case, both the normal and the shear forces contribute to the particle crushing and affects the observed force-displacement response. However, the average peak force, F_c , of a group size causing the major breakage of the glass sphere increases with the mean equivalent area diameter of the glass spheres (Figure 4.2).



(a)



(b)

Fig. 4.1. Typical force-displacement response for glass sphere particles: (a) 2.5mm diameter group and (b) 6mm diameter group

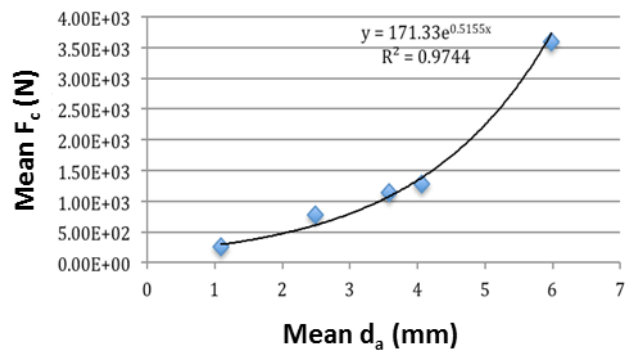


Fig. 4.2. Relation between the crushing force, F_c , and mean equivalent area diameter, d_a , of glass sphere particles

For a given vertical force, the tensile stress developed in the particle σ is proportional to F/d^2 , where d is the particle diameter, [30], in this case assumed equal to d_a . The critical tensile stress decreases with the increasing of the size of the glass sphere, but the rate of decrease reduces for particle sizes higher than 4 mm (Figure 4.3).

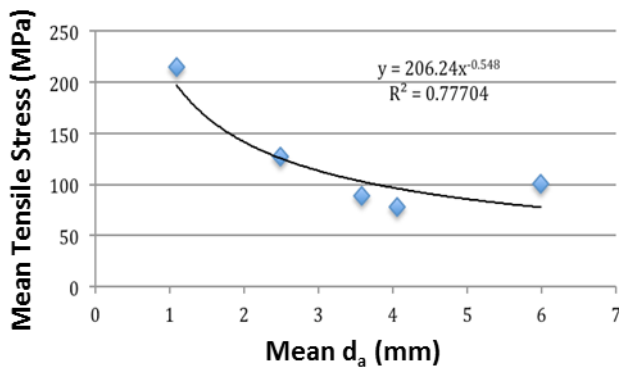


Fig. 4.3. Tensile stress- d_a of glass crushing tests

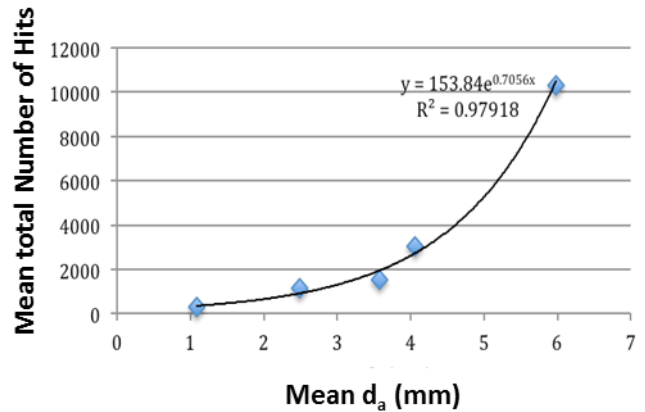


Fig. 4.5. Average of total AE Hits function of the d_a of glass spheres

B. AE analysis

Typical acoustic emission activity detected during a crushing test of a glass particle is illustrated in Figure 4.4 where the calculated Energy - integral of the rectified voltage signal over the duration of the AE signal - of each recorded AE event is superimposed over the vertical force response. With the exception of the particle crushing point where the released energy reaches a clear and distinct peak, the intensity of the AE activity is relatively low throughout the loading test (the initial AE signals recorded at the beginning of the test are rather assigned to the mechanical set up of the contacts between the platens and the particle).

The number of pulses that exceed the detection threshold, hits (Figure 3.2), have been counted for the all the AE events recorded during a test and the variation of the average number of hits per each group size function of the particle group sizes is shown in the Figure 4.5. It is clearly observed that the higher the particle size is, the larger is the number of hits of the acoustic emission signals.

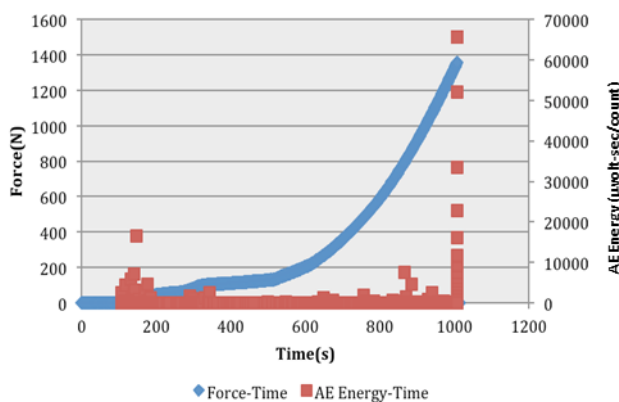
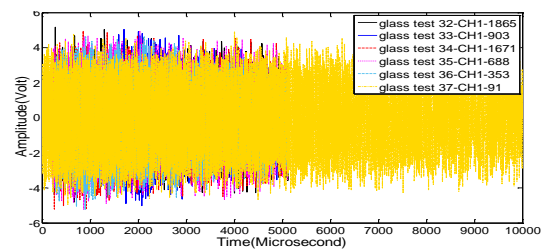
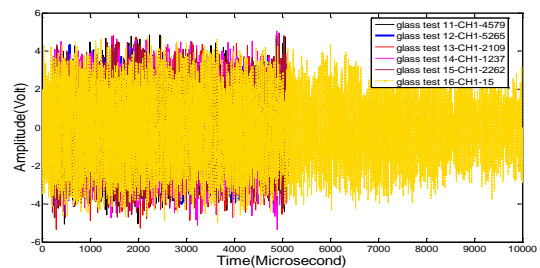


Fig. 4.4. Typical Force-AE Energy-Time response recorded during a crushing test of a glass sphere

Typical ‘crushing’ signals for 2.5 mm and 4 mm particle size diameters, are shown as an example in Figure 4.6. The analysis of the AE waveform signals shows some interesting results. First, the maximum amplitude (positive or negative) of the signals does not appear to be affected by the size of the particles and systematically reached a value around 114 dB. Figure 4.7 presents the values of the calculated mean Absolute Energy - integral of the squared voltage signal divided by the reference resistance (10k-ohm) - for each particle size group. At the crushing point, the Absolute Energy of the recorded signals appears rather unchanged for low particle size diameters whereas some dependency is clearly observed for particle diameters higher than 4 mm.



(a)



(b)

Fig. 4.6. AE waveform recorded at the crushing point for several particles of (a) 2.5 mm and (b) 4 mm average size diameters

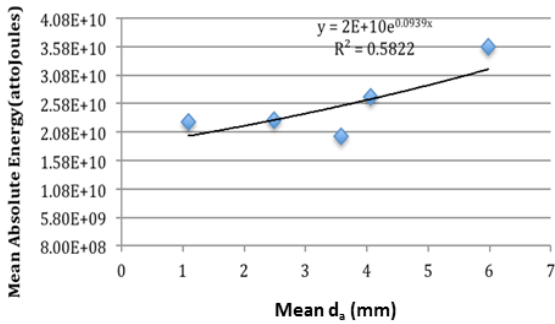


Fig. 4.7. Mean Absolute Energy versus d_a of glass spheres

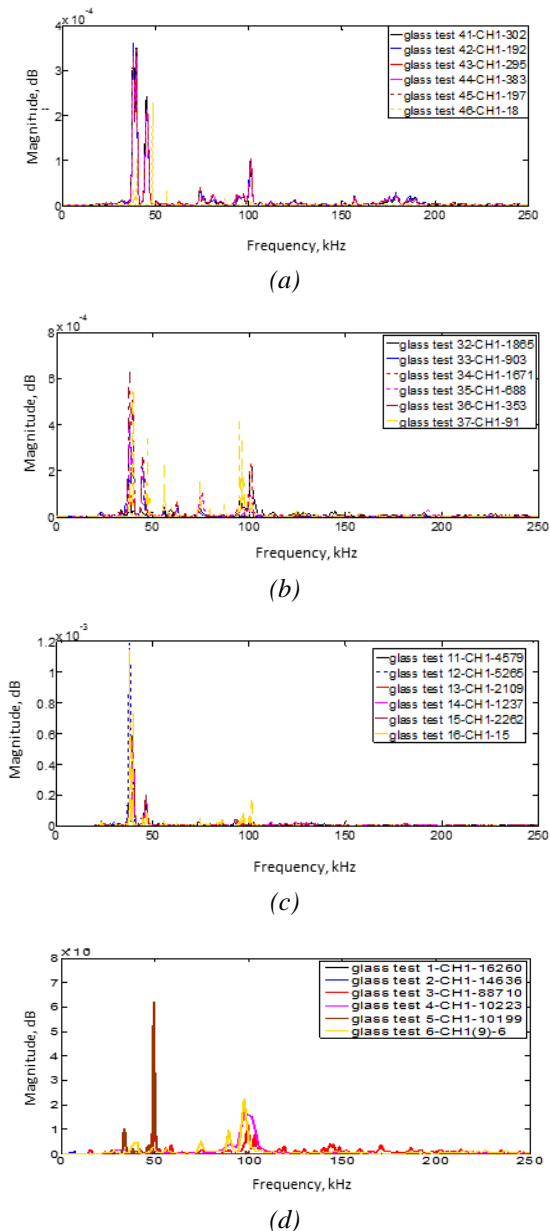


Fig. 4.8. Power spectra density estimates of the AE signals for (a) 1mm, (b) 2.5mm, (c) 4mm and (d) 6mm particle sizes

C. Frequency domain analysis of AE signals

The analysis of the AE signals in the frequency domain is based on Welch's power spectral density estimate method [31] and was conducted using Matlab software package [32]. The power spectra density estimates of the AE signals for 1 mm, 2.5 mm, 4 mm and 6 mm size groups are shown in the Figure 4.8. The peaks in the power spectra densities for all the particles seem to appear at almost identical frequencies around 38 KHz, 45 KHz, 75 KHz and 100 KHz. These results suggest that the AE signals recorded at the final crushing point are mainly linked to a typical particle breakage mechanism, in this case glass particles disintegrate instantly into small pieces. The AE can provide the signature of a crushing type. However, AE signal parameters like Absolute Energy show some particle size dependency and these can be used to discriminate between different particle size types if AE measurements are conducted on samples of agglomerates of particles.

V. CONCLUSION

This study explored the possibility of using Acoustic Emission technique as a passive method to characterize the extent of soil particle breakage and predict its particle size evolution under loading. For this purpose, at this stage, individual glass spherical particles – analogue granular soil particles - of various sizes have been loaded up to failure under uniaxial compression conditions. The main focus was to detect the particle's AE signature that can subsequently be used in tests of bulk agglomerates of particles to discriminate between AE events and get insight into the individual breakage mechanisms.

AE signal events are clearly recorded at the breaking point of the individual particles and the account of various AE signal parameters show some dependency with the variation of the particle size. In contrast, the frequency content of the AE signals at the failure point does not appear to be affected by the particle size and that suggests that the AE can be directly linked to a typical particle breakage mechanism. At the breakage point all the glass particles crush in a similar way by instantly disintegrating into small pieces. Further studies on different types of particles like chalk, silica, salt are in progress, including measurements on samples formed by different size particles.

REFERENCES

- [1] Covarrubias SW, 1969. "Cracking of Earth and Rockfill Dams", H Harvard University Press: Cambridge, Massachusetts, 1969 , vol. 82, 123.
- [2] Sherard JL , "Embankment dam cracking", In

Embankment Dam Engineering, Hirschfeld RC, Poulos SJ (eds). Wiley: New York, 1973, 271–353.

- [3] Dai ST, Labuz JF. 1997. “Damage and failure analysis of brittle materials by acoustic emission”. *J Mater Civil Eng.*, vol. 9(4): 200-205.
- [4] Yuyama S, Okamoto T, Nagataki S, 1994. “Acoustic emission evaluation of structural integrity in repaired reinforced concrete beams”, *Material Evaluation*, vol. 52(1), 88-90.
- [5] Giordano M, Calabro A, Esposito C, D’Amore A, Nicolais L., 1998, “An acoustic-emission characterization of the failure modes in polymer–composite materials”, *Compos Sci Technol*, vol. 58, 1923–1928.
- [6] Bohse J. 2000, “Acoustic emission characteristics of micro-failure processes in polymer blends and composites”, *Compos Sci Technol*, vol. 60, 1213–1226.
- [7] Huguet S, Godin N, Gaertner R, Salmon L, Villard D. , 2002. “Use of acoustic emission to identify damage modes in glass fibre reinforced polyester”, *Compos Sci Technol*, vol. 62, 1433–1444.
- [8] Haselbach W, Lauke B., 2003. “Acoustic emission of debonding between fibre and matrix to evaluate local adhesion”, *Composite Science Technology*, vol. 63(15), 2155–2162.
- [9] Shigeishi, M., Colombo, S., Broughton, K.J., Rutledge, H., Batchelor, A.J., Forde, M.C., 2001. “Acoustic emission to assess and monitor the integrity of bridges.” *Construction and Building Materials*, 15, 35-49.
- [10] Lord, A.E., Koerner, R.M., 1974. “Acoustic-emission response of dry soils.” *Journal of Testing and Evaluation* 2, 159–162.
- [11] Lord, A.E., Koerner, R.M., 1975. “Acoustic emissions in soils and their use in assessing earth dam stability.” *Journal of the Acoustical Society of America* 57, 516–519.
- [12] Koerner, R., Lord, A., McCabe, W., Curran, J., 1976. “Acoustic-emission behavior of granular soils” *Journal of the Geotechnical Engineering Division – ASCE* 103, 1460–1461.
- [13] Koerner, R.M., Lord, A.E., McCabe, W.M., 1977. “Acoustic-emission behavior of cohesive soils.” *Journal of the Geotechnical Engineering Division – ASCE* 103, 837–850.
- [14] Chichibu, A., Jo, K., Nakamura, M., Goto, T., Kamata, M., 1989. “Acoustic emission characteristics of unstable slopes.” *Journal of Acoustic Emission* 8, 107–111
- [15] Rouse, C., Styles, P., Wilson, S., 1991. “Microseismic emissions from flowslide-type movements in South Wales.” *Engineering Geology* 31, 91–110.
- [16] Dixon, N., Hill, R., Kavanagh, J., 2003. “Acoustic emission monitoring of slope instability: Development of an active waveguide system.” *Proceedings of the ICE: Geotechnical Engineering* 156, 83–95.
- [17] Dixon, N., Spriggs, M., 2007. “Quantification of slope displacement rates using acoustic emission monitoring.” *Canadian Geotechnical Journal* 44, 966–976.
- [18] Tanimoto, K., Nakamura, J., 1981. “Studies of acoustic emission in soil.” In: Drnevich, V.P., Gray, R.E. (Eds.), *Acoustic Emission in Geotechnical Engineering Practice*, ASTM STP 750. American Society for Testing and Materials, pp. 164–173
- [19] Fernandes, F., Syahrial, A.I., Valdes, J.R., 2010. “Monitoring the oedometric compression of sands with acoustic emissions.” *Geotechnical Testing Journal*, American Society for Testing and Materials 33, 410–415.
- [20] Wang, Y., Ma, C., Yan, W., 2009. “Characterizing bond breakages in cemented sands using a mems accelerometer.” *Geotechnical Testing Journal* 32, 1–10
- [21] Karner, S.L., Chester, F.M., Kronenberg, A.K., Chester, J.S., 2003. “Subcritical compaction and yielding of granular quartz sand.” *Tectonophysics* 377, 357–381
- [22] Villet, W., Mitchell, J., Tringale, P., 1981. “Acoustic emissions generated during the quasistatic cone penetration of soils.” In: Drnevich, V.P., Gray, R.E. (Eds.), *Acoustic Emission in Geotechnical Engineering Practice*, ASTM STP 750. American Society for Testing and Materials, pp. 175–193
- [23] Aslan, H., and Baykal, G. 2006 “Analysisng the crushing of granular materials by sound analysis technique.” *Journal of testing and Evaluation*, vol. 34, No. 6, 1-7

- [24] Cavarretta, I., O’Sullivan, C., Ibraim, E., Martin Lings, M., Hamlin, S., Muir Wood, D. 2012. “Characterization of artificial spherical particles for DEM validation studies.” *Particuology* 10, 209–220
- [25] Wadell, H. 1932. “Volume, shape, and roundness of rock particles.” *Journal of Geology*, 40, 443–451.
- [26] Wadell, H. 1933. “Sphericity and roundness of rock particles.” *Journal of Geology*, 41, 310–330.
- [27] ISO, ISO 9276-6:2008(E), “Representation of results of particle size analysis — Part 6: Descriptive and quantitative representation of particle shape and morphology”, 2008
- [28] Cavarretta, I., O’Sullivan, C., & Coop, M. 2009. “Applying 2D shape analysis techniques to granular materials with 3D particle geometries.” In *Powders and grains 2009: Proceedings of the 6th international conference on micromechanics of granular media* Vol. 1145(1), 833–836.
- [29] Cavarretta, I., and O’Sullivan, C. 2012. “The mechanics of rigid irregular particles subject to uniaxial compression.” *Géotechnique*, 62(8), 681-692
- [30] Jaeger, J. C, 1967. “Failure of rocks under tensile conditions.”, *Int. J. Rock. Min. Science*, vol. 4, 219-227.
- [31] Welch, PD. 1967. “The Use of Fast Fourier Transform for the Estimation of Power Spectra: A Method Based on Time Averaging Over Short, Modified Periodograms.” *IEEE Transactions on audio and electroacoustics*, Vol. AU-15, No. 2.
- [32] MATLAB (The language of technical computing), 7 ed: The Mathworks Inc, 2010